Biomass Conversion and Biorefinery
https://doi.org/10.1007/s13399-024-05566-6

ORIGINAL ARTICLE

A novel additive for enhancing biomass energy production from agro-industrial wastes: synthesis of hydrophobic nanoporous silica aerogel and its effect on methane production

Habibe Elif Gulsen Akbay[1] · **Oykum Basgoz**[2] · **Omer Guler**[3]

Received: 5 January 2024 / Revised: 13 March 2024 / Accepted: 26 March 2024

Abstract

Anaerobic digestion (AD) is one of the most preferred processes for the treatment of organic waste. However, additional processes such as co-digestion, pretreatment, and additive addition continue to be explored to remove the limits on the applicability of AD. This study investigated the effects of hydrophobic nanoporous silica aerogel (NpSA) synthesized from waste rice husks on the anaerobic co-digestion (AnCD) of the mixture consisting of sewage sludge and fruit processing industry wastes. All bioreactors containing NpSA-free, 0.1 g, 0.2 g, 0.5 g, and 1 g NpSA (0.03–0.3 g_{NpSA}/gVS_{added}) were operated in a mesophilic-batch process. Biogas and methane yields increased from 346 mL/gVS (NpSA-free) to 387 mL/gVS and from 231 mL/gVS (NpSA-free) to 288 mL/gVS, respectively, with 0.1 g NpSA addition. NpSA additive increased biogas production in all bioreactors compared to the blank. However, biogas production rate and methane content increased faster at lower doses of NpSA. Maximum soluble chemical oxygen demand (sCOD), protein, carbohydrate, and volatile solid (VS) reductions were between 45–71%, 35–54%, 44–65%, and 34–91% for NpSA added mixtures, respectively. The hydrophobic NpSA additive was effective in improving the AnCD performance and biogas/methane production. Experimental results fit the kinetic models frequently preferred in such AD processes. In addition, the possible energy and financial potential of the produced methane were also discussed, and it was determined that the direct sale of methane gas produced by the addition of NpSA in the global market could provide 1.4 $/$L_{mixture}$ more financial gain than the mixture NpSA-free.

Keywords Anaerobic digestion · Biomass energy · Industrial waste · Rice husk · Sewage sludge · Silica aerogel

Highlights
- Hydrophobic nanoporous silica aerogel was synthesized from rice husk ash in a new way.
- Nanoporous silica aerogel acted as a catalyst in organic matter degradation.
- Lower doses of NpSA led to a greater increase in biogas production than higher doses.
- Methanogenesis occurred in a shorter time with less NpSA dose and the CH_4 yield was 75% on average.
- NpSA as an additive improved microbial activity and shortened the lag phase time.

✉ Habibe Elif Gulsen Akbay
elifgulsen@mersin.edu.tr

[1] Department of Environmental Engineering, Mersin University, Mersin 33343, Turkey

[2] Department of Metallurgical and Material Engineering, Mersin University, Mersin 33343, Turkey

[3] Rare Earth Elements Application and Research Center, Munzur University, Tunceli 62000, Turkey

1 Introduction

Increasing population and economic and technological developments cause an energy crisis worldwide and increase the use of unsustainable fossil fuels that cause environmental pollution [1–4]. This global energy consumption is projected to increase by 50% between 2020 and 2050 [1]. For this reason, energy sectors attach importance to studies and developments on renewable energy sources that will replace fossil fuels.

Different technologies and processes contribute to renewable and sustainable energy requirements, such as biomass, hydroelectric, geothermal, solar, wind, and ocean (tidal and wave) energy [5–7]. Among these, biomass energy comes to the forefront due to the reduction of greenhouse gases and, at the same time, the removal of organic waste from landfills and its high calorific value [8].

Managing domestic and industrial solid wastes and the organic fraction of large volumes of sewage sludge produced

Published online: 13 April 2024

by wastewater treatment plants (WWTP) are among the important environmental issues [9–11]. Anaerobic digestion (AD) is a widely used method that allows biodegrading organic materials in such wastes and converting them into an energy source such as biogas [12, 13]. Today, wastes are evaluated through anaerobic co-digestion (AnCD) processes to increase the methane content of biogas, which generally consists of 50–70% methane (CH_4), and to ensure sustainable production [14–16]. Although the development and widespread use of technological activities related to the AD process has increased, some deficiencies such as the low biodegradation efficiency of the wastes/substrates used in the process, environmental factors, and difficulties encountered in stabilization of the system limit the industrial and commercial application of the AD process. Numerous pretreatment methods such as physical, chemical, biological, and hybrid have been investigated to overcome such drawbacks [17]. However, the use of additives (biochar, nanoparticles, chemicals, aerogels, etc.) that allow anaerobic microorganisms to adhere to the environment for rapid growing reduces the lag phase, and rapid substrate hydrolysis, thanks to their large surface area in AD processes, is a promising application for system stability and efficiency. Thus, biogas production can increase, and impurities in gaseous form in the produced biogas can also be removed [18].

In literature studies, it has been reported that additives, which attract attention with their positive contributions to the AD process, affect biogas and methane production depending on various factors such as specific surface area, porosity, pore size, abundance, and surface roughness [19–21]. Some of these additives represent materials such as polyurethane foam, vegetal carbon [22], carbon [21], zeolite [23], silica gel [24], nano metal [25], street dust [26], slag [27], and biochar [28]. For instance, Picanco et al. [29] and Breitenbucher et al. [30] studied the effect of material porosity on anaerobic biomass adhesion. They reported that a large surface area is a crucial requirement for the adhesion of large amounts of biomass. In this context, the additive material to be used to increase the adhesion surface of anaerobic microorganisms in a successful AD system needs properties such as having a large surface area, being porous, and being stable [31]. The additive that is added to the bioreactor indirectly determines the biomass holding capacity, and therefore, selecting a suitable additive is very important to ensure the success of the process [32].

Aerogels, which have become widely used as additives recently are used in adsorption, thermal insulation, catalysis, and other fields due to their superior properties such as large specific surface area (500–1200 m^2/g), porous structure, and good adsorption performance [33]. The most important issue in the production of silica aerogels is the removal of solvents trapped in the pores from the wet gel structure by the sol–gel method without damaging the 3D network of the aerogel [34]. The conventional method for removing solvent from wet gel is a supercritical drying procedure involving a complex and dangerous process [35]. This hazardous and costly method limits the large-scale production of silica aerogels and their wide use in various potential applications. In this study, the drying step was carried out in the ambient atmosphere instead of a supercritical drying procedure to reduce this hazardous effect. Also to reduce the high cost, which is one of the handicaps of silica aerogel production, waste rice husk was used as a precursor in the synthesis process, and thus stable and hydrophobic nano-porous silica aerogel (NpSA) was synthesized. In addition, a trace amount tetraethyl orthosilicate (TEOS) was used together with polydimethylsiloxane (PDMS) before gelation to contribute to the permeability properties of PDMS molecules, show thermal stability and contribute to hydrophobicity, and strengthen the 3D network structure of silica gel.

The synthesized NpSA was then used to fill the research gap on the use of NpSA to enhance biogas/methane production in the AD process by adding it to a mixture of pomegranate juice production waste and domestic sewage sludge, whose biogas and methane production efficiency was proven and optimized in a previous study [36]. The effects of NpSA added to this mixture at certain doses on biogas/methane production and dissolved organic matter removal in the environment were investigated. Thus, it aims to examine the effects of silica aerogel additive and dose on increasing biogas yields and obtaining high methane rate more quickly in equal digestion time in food industries and sewage sludge generating processes. In addition, methane production in all bioreactors was evaluated by kinetic modeling studies to provide a complete perspective on the effect of NpSA on the AnCD mechanism. However, based on the cost being one of the driving forces for applying new technology to increase energy efficiency in such processes, an energy and financial evaluation related to methane production efficiency was also made to concretely determine the potential benefits of NpSA.

2 Materials and methods

2.1 Synthesis of hydrophobic NpSA

2.1.1 Synthesis materials

Rice husk (RH) was obtained from the "Tat Bakliyat" company in Mersin, Turkey. In NpSA production, hydrochloric acid (HCl) (Merck), sodium hydroxide pellet (NaOH) (Merck), sulfuric acid (H_2SO_4) (Merck), tetraethylorthosilicate (TEOS) (Merck), polydimethylsiloxane (PDMS) (Merck), ethyl alcohol (EtOH) (Sigma-Aldrich), ammonium

hydroxide (NH_4OH) (Sigma-Aldrich), and n-hexane (Merck) chemicals were used.

2.1.2 Synthesis procedure

NpSA synthesis was carried out using the sol–gel method. In this method, sodium silicate (Na_2SiO_3) solution, which was synthesized from rice husk ash (RHA), was used as a precursor. Leaching was carried out with RH 0.5 M HCl. After acid leaching, RH was washed with distilled water and calcined gradually at 600 °C for 4 h (waiting 50 min per 100 °C until 600 °C) to obtain RHA. Ten grams of RHA was dissolved in 1 mol/L NaOH aqueous solution at 100 °C for 1.5 h. The mixture was then filtered under a vacuum to remove undissolved residues. The liquid (Na_2SiO_3 solution) passing through the filter was neutralized at pH:7 with 0.25 mol/L H_2SO_4 to form silica hydrogel. At this stage, TEOS was used with PDMS before gelation (post-gelation) to strengthen the silica gel's three-dimensional (3D) network structure. TEOS + PDMS solvent 1:1.2 by volume was used. The prepared gel was aged in NHOH for 24 h at 60 °C. To remove the sodium sulfate formed after the neutralization process, the aged gel was washed five times, every 4 h, with EtOH/H_2O solution. The silica gel was soaked in TMCS:n-Hexane:EtOH solution for three days to drain the H_2O/EtOH solutions in the pores and to modify the surface. This solution was renewed every 12 h. Mass transfer in the gel was realized only by diffusion, and surface modification processes were carried out after silica gel formation. Gradual drying was carried out in an ambient atmosphere for 2 h at 50 °C, 2 h at 90 °C, and 1 h at 120 °C. Hydrophobic NpSA synthesis flow diagram is given in Fig. 1.

2.1.3 Characterization of hydrophobic NpSA

Elemental characterization of RHA was determined by X-ray fluorescence spectrometer (XRF) (Rigaku ZSX Primus II); NpSA's surface area measurements and pore distribution were analyzed by Branuer, Emmet, and Teller (BET) surface area measurement (Micrometrics Surface Area and Porosity, TriStar II), respectively. Hydrophobicity and microstructure examination of NpSA were determined by using a water contact angle meter (Attension Theta Flex) and a scanning electron microscope (FEI, Nova NanoSEM 450), respectively.

2.2 Anaerobic co-digestion process

2.2.1 Substrates and inoculum

Pomegranate waste (PW) and pomegranate wastewater (PWW) were taken from a major producer of fruit juice concentrates, fruit purees/pulp, and aromas/flavors in Mersin, Turkey. Sewage sludge (SS) was taken from a WWTP in Karaduvar, Mersin. Both solid wastes (PW and SS) were dried in an oven at 60 °C for 24 h [37]. After reaching the ambient temperature in the desiccator, both were crushed with a household grinder to a maximum particle size of 0.5 mm. The ground substrates were stored in a desiccator. Fresh cattle manure with 21% TS was used for bacterial inoculation. The bacterial inoculum was prepared as previously described [38].

2.2.2 Experimental setup of AnCD

The results of a previous study were evaluated for the base mixture prepared with the aim of investigating the effect of the abundance ratio of NpSA in the mixture on AnCD process. According to the results of a previous study conducted by mixing different fruit wastes (pomegranate, apple, and black carrot) with sewage sludge in equal proportions (% on TS basis), the highest biogas production was obtained in bioreactors with PW and SS. The biogas production (on a ml/gVS basis) of the mixture containing PW was 22% and 19% higher than the mixtures containing apple waste and carrot waste, respectively [36]. Therefore, in the continuation of this study, the possibility of enhancing biogas production using pomegranate and sewage sludge with the addition of NpSA was investigated.

Batch AnCD experiments were performed in 125-mL glass bioreactors (working volume 50 mL) which has rubber septum for gas sampling. Dry waste mixtures (%4TS PW-4%TS SS) were diluted with PWW to make the final TS ratio in the bioreactors 8%. Then, bacterial inoculum was added to each bioreactor, representing 8% of the total working volume (4 mL). The initial pH values of the mixtures were fixed at 7.6 ± 0.2 with $NaHCO_3$ solution, with the privilege of contributing positively to the biogas production of the alkalinity parameter. Finally, NpSA was loaded into the bioreactors with a different abundance of 0, 2, 4, 10, and 20 $g/L_{mixture}$ as displayed in the "supplementary material (SM. Table 1)." After the preparation of the mixtures, the bioreactors were closed with a rubber septum, and the environment was deprived of oxygen by scavenging with nitrogen gas for 120 s (99.99% purity) using a double injector. Finally, the bioreactors were placed in the incubator with a shaking speed of 150 rpm and the temperature was fixed to be mesophilic (37 ± 1 °C). Biogas formation in the bioreactors was monitored until it showed a steady decrease (for 60 days). The daily volume of biogas was determined by the water displacement method. The percentage of methane was analyzed every 5 days by adsorbing the CO_2 in the known volume of biogas with KOH solution [39, 40]. Triplicate bioreactors were used in all experimental sets and all values were means of triplicates ± standard deviation.

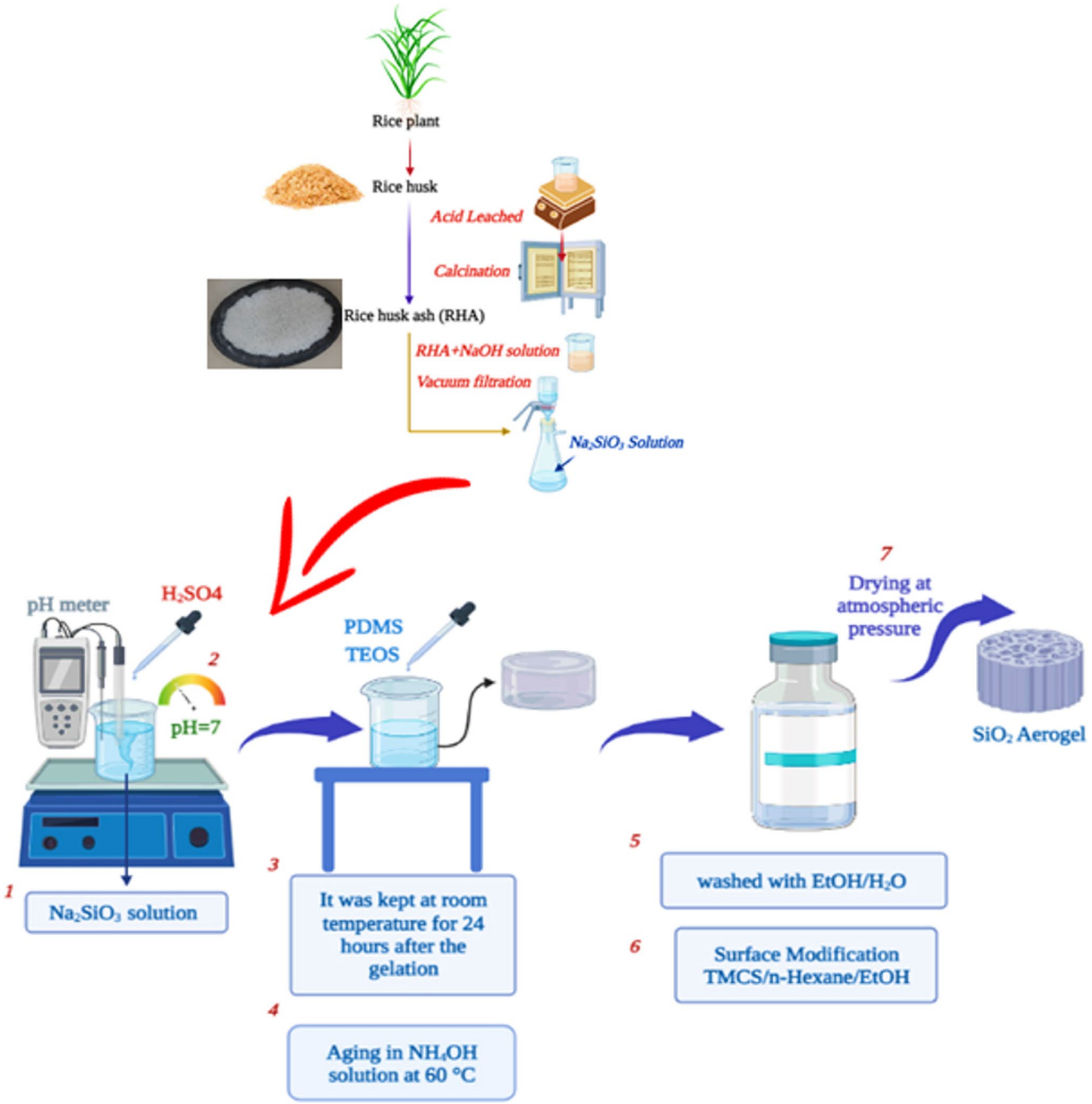

Fig. 1 The hydrophobic NpSA synthesis flow diagram

2.2.3 Analytical methods

Initial pH, total solids (TS), and volatile solids (VS) of the feedstock and substrates were analyzed according to standard methods [41–43]. Chemical oxygen demand (COD) was determined by closed reflux titrimetric method [44]. Carbohydrate and protein concentrations were analyzed by phenol sulfuric acid [45] and the Lowry [46] methods, respectively. The basic characteristics of the raw substrates (PW, PWW, and SS) and the main mixture with 8%TS content (NPSA-free) subsequently used for AnCD are given in Table 1. The solubility of organic matters (COD, carbohydrates, and proteins) was analyzed before and after AnCD by the method given previously [38]. Reduce in soluble organic matter (sOM) and VS concentrations after AnCD was calculated by Eq. (1) and Eq. (2) [38]. Each sample was analyzed in triplicate.

Table 1 Basic characteristics of raw substrates and main substrate mixture

Parameter	Unit	Raw substrates			Main mixture (NpSA-free %8 TS)
		Pomegranate wastewater (PWW)	Pomegranate waste (PW)	Sewage sludge (SS)	
pH	–	5.42 ± 0.02	3.27 ± 0.03	7.78 ± 0.01	5.62 ± 0.02
Total solids (TS)	mg/L or gTS/$kg_{rawwaste}$	2820 ± 20	266.66 ± 4.5 (%27)	269.58 ± 2.6 (%27)	8%
Volatile solids (VS)	gVS/kgTS	–	686.25 ± 4 (%68)	403.80 ± 3 (%40)	4% (TS basis)
	$mg/L_{feedstock}$	–	–	–	61.9
Total COD (TCOD)	mg/L	2027 ± 8	58,000 ± 160	28,800 ± 110	62,000 ± 120
Soluble carbohydrate (sCH)	mg/L	384.72 ± 5	8428 ± 34.6	217.58 ± 14.8	17,142 ± 38.5
Soluble protein (sPT)	mg/L	402.48 ± 12.6	6200 ± 28.4	396.86 ± 9.4	6351 ± 32.6
Soluble COD (sCOD)	mg/L	–	32,000 ± 152.6	1200 ± 84.2	28,480 ± 108.3
C/N	%	–	46.98	8.29	27.63

$$Removal\ of\ sOM\% = \frac{\left(sOM_{initial} - sOM_{anaerobic\ digested}\right)}{sOM_{initial}} * 100 \quad (1)$$

$$Removal\ of\ VS\% = \frac{\left(VS_{initial} - VS_{anaerobic\ digested}\right)}{VS_{initial}} * 100 \quad (2)$$

The functional groups of the main feedstock and feedstocks added NpSA were analyzed with the FT-IR instrument (Perkin Elmer) after AnCD process (digestates). In addition, total carbon (C) and total nitrogen (N) values (%) of the substrates were determined by an elemental analyzer (Thermo Fisher Scientific Flash 2000).

2.3 Kinetic study

As a result of the mathematical definition of the amount of methane produced by AnCD using different kinetic models, an evaluation can be made about the hydrolysis rate of organic matter in the mixture and the lag phase, which provides information about the start of biogas production in the bioreactor. In this study, equations modeled in nonlinear curve fitting mode using OriginPro (2021) are given in Table 2.

Both the correlation coefficients (R^2) and the root mean square error (RMSE) values were determined with the Eq. (3) to interpret the closeness of the experimental results (actual value) with the kinetic model results (estimated value) and to make predictions about the model success [50].

$$\mathrm{RMSE} = \sqrt{\frac{\sum_{i=1}^{N}\left(Y_{pre,i} - Y_{exp,i}\right)^2}{N}} \quad (3)$$

where $Y_{pre,i}$ is the methane yield predicted by the model, and $Y_{exp,i}is$ the mean methane yield calculated in the AnCD experiments. Also, "N" represents a set of data points.

2.4 Energy potential and financial profits

The energy conversion (EN_{out}) of the amount of methane produced in each bioreactor after AnCD and the financial gain (F_{gain}) that can be obtained from electrical energy consumption thanks to this conversion were calculated by Eq. (4) and Eq. (5), respectively [51].

$$EN_{out} = \left(Y_{CH_4} * \xi\right) \div 1000 \quad (4)$$

$$F_{gain} = EN_{out} * P_E * 0.000278 \quad (5)$$

where Y_{CH_4} is the CH_4 yield after each AnCD experiment (mL/gVS) and ξ is the lower heating value of CH_4 (35.8 kJ/L); P_E is the worldwide average price of electricity,

Table 2 The kinetic models used in this study

Kinetic model	Equation	Abbreviations	Ref
Modified Gompertz	$C(t) = U * \exp\left(-exp\left(\left(Rb * \frac{2.7183}{U}\right) * (\lambda - t) + 1\right)\right)$	$C(t)$: cumulative methane production (mL/gVS) U: ultimate methane production potential (mL/gVS) R_b: maximal methane production rate (mL/g VS·day) λ : lag phase time (days) t: time in days $exp\ (1) = 2.7183$	[47]
Transference function	$C(t) = U * \left\{1 - exp\left(-\frac{Rb*(t-\lambda)}{U}\right)\right\}$		[48]
Logistic function	$C(t) = \frac{U}{1+exp\left\{4R_b * \frac{(\lambda-t)}{U} + 2\right\}}$		[49]

$0.165/kWh [52], and "0.000278" is the conversion factor of kilojoule to kilowatt per hour.

In addition to the energy conversion, the financial profit can be obtained by directly selling the methane (S_M) produced in bioreactors as gas on the world market calculated by using Eq. (6).

$$S_M = \left(P_{CH_4} * P_M\right) \div 1000 \quad (6)$$

where P_{CH_4} is the methane yield after AnCD experiments (mL/gVS) and P_M is the mean price of $CH_{4(gas)}$ worldwide: $1.24/L [53].

3 Results and discussion

3.1 Characterization of hydrophobic NpSA

Sodium silicate synthesized from RHA was used as a precursor in the synthesis of NpSA according to the experimental procedure given in Section 2.1.2. It is essential that RHA contains high-purity SiO_2 for the quality of the synthesized sodium silicate solution. Therefore, XRF analysis was executed on RHA after calcination and chemical leaching, and the results of this analysis are given in Table 3. According to the XRF analysis results, RHA contains 92% SiO_2 after washing with pure water + calcination. NpSA, dried in an ambient atmosphere, has hydrophobic properties and a porous structure. After acid leaching, impurities such as iron (III) oxide (Fe_2O_3), aluminum oxide (Al_2O_3), magnesium oxide (MgO), and calcium oxide (CaO) and, more importantly, detrimental alkalis such as sodium (Na_2O) and potassium oxide (K_2O) are released into RHA. Finally, % RHA value was determined as 98% SiO_2 according to XRF elemental analysis (Table 3).

Table 3 The result of XRF analysis of the RHA washed with pure water after calcination and leaching

Chemical content	Washing with distilled water + calcination	Washing with distilled water + chemical leaching
SiO_2	92.075	98.53
Na_2O	0.303	0.124
MgO	0.618	0.235
Al_2O_3	0.2466	0.085
P_2O_5	0.5309	0.0813
SO_3	0.4753	0.399
Cl	0.2092	0.0053
K_2O	2.9506	0.0243
CaO	1.395	0.345
Cr_2O_3	0.0849	0.0037
MnO	0.0662	0.0054
Fe_2O_3	0.7884	0.123
ZnO	0.0074	0.0117
Other	0.1829	0.0093

Characterization results of NpSA are given in Fig. 2, SEM image of NpSA is provided in Fig. 2a. The contact angle measurement result of NpSA is shown in Fig. 2b. Barrett-Joyner-Halenda (BJH) pore size distribution graph of NpSA is given in Fig. 2c and the N_2 adsorption/desorption BET isotherm graph obtained at 77 K in Fig. 2d. Before the BET analysis, the NpSA sample to be analyzed was degassed under a vacuum at 150 °C for 3 h to remove the physically bound impurities on the surface of the aerogel. Cumulative pore volume (cm^3/g) and average pore diameter (nm) were determined using the BJH adsorption cumulative pore volume method. The results of the FT-IR analysis to characterize the chemical composition and interactions of the functional groups in hydrophobic NpSA are given in Fig. 2. The SEM image showing the morphological structure of NpSA is given in Fig. 2a; it is seen that NpSA has a continuous 3D porous network structure and has been successfully synthesized.

According to the image given in Fig. 2b, it is seen that the water droplet stops on the surface of NpSA with an average contact angle of 150.40°. This shows that the synthesized NpSA has a hydrophobic character. According to the BJH pore size distribution graph in Fig. 2c, the pore volume and average pore diameter values are 0.301981cm^3/g and 4.32 nm, respectively. According to the BET isotherm graph given in Fig. 2d, the surface area of NpSA is 513.023 surface m^2/g. The BET isotherm plot shows that the structure is mesoporous and conforms to Type-IV, which represents mesoporous materials, according to the International Union of Pure and Applied Chemistry (IUPAC) classification.

As a result of the characterization analyses, it was thought that the synthesized NpSA could provide an advantage to the growth and reproduction activities of anaerobic microorganisms by increasing their adhesion to this structure surface, thanks to its porous and large surface area. In addition, it was concluded that the hydrophobicity of NPSA is advantageous in terms of maintaining the stability of the substrate mixture in the bioreactor. Thus, it was thought that it could act as a catalyst in dissolving the organics that need to be dissolved in the mixture in the bioreactor by pushing the liquid into the environment. Besides, it was concluded that thanks to the functional groups on its surface, it can contribute to increasing the methane production potential by adsorbing the CO_2 in the biogas produced by AD.

3.2 Biogas and methane production

The daily and cumulative biogas production potential of AnCD of mixtures containing NpSA in different abundances and NpSA-free (blank) is given in Fig. 3. Cumulative methane production and content of methane (CH_4%) for

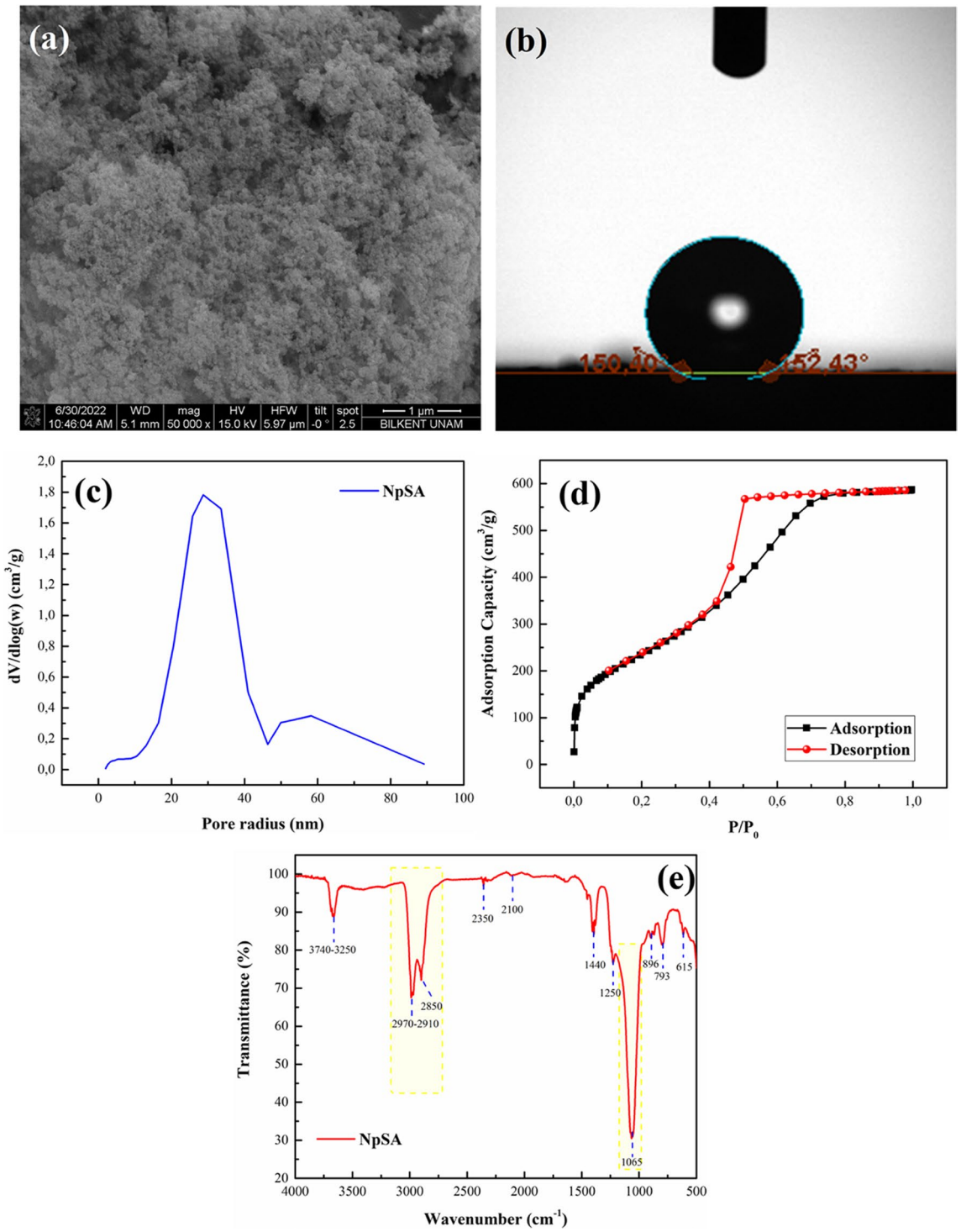

Fig. 2 SEM microstructure image of NpSA (**a**), contact angle measurement result (**b**), BJH pore size distribution graph (**c**), N_2 adsorption/desorption BET isotherm graph (**d**), FT-IR analysis (**e**)

all bioreactors are shown in Fig. 4. The cumulative biogas production of NpSA-free mixture was 1070.5 mL (Fig. 3a), corresponding to the lowest biogas production achieved during the study. The cumulative biogas production efficiencies of the mixtures containing NpSA, from the lowest to the highest dose, were 1198.5 mL, 1153.5 mL, 1162 mL, and 1171 mL, respectively. At the end of the 60-day experimental period, the biogas production efficiency of the bioreactors

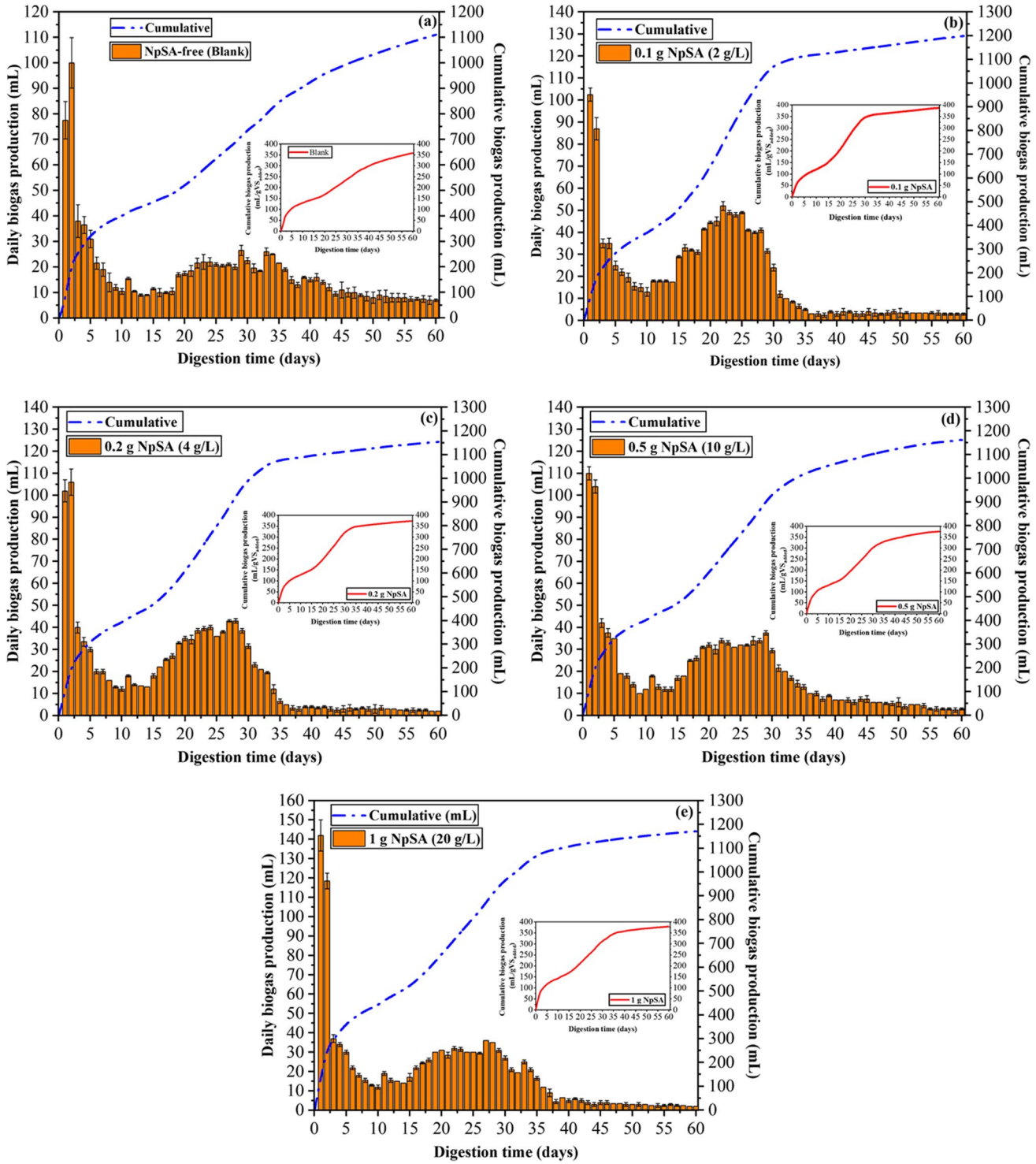

Fig. 3 Cumulative and daily biogas production of NpSA-free (**a**), 0.1 g NpSA (**b**), 0.2 g NpSA (**c**), 0.5 g NpSA (**d**), and 1 g NpSA (**e**)

containing NpSA increased by an average of 8–12% compared to the mixture without NpSA. Similarly, in a 76-day batch AD system study investigating the effect of silica gel catalyst on the biogas production potential of cow manure under mesophilic conditions, it was reported that an 11.94% increase in total gas production was observed with the addition of 2.8 g silica gel catalyst (4 g/$L_{mixture}$) to the medium (7–9% TS) [54].

When Fig. 3 was examined carefully, it was seen that the daily biogas production efficiency of mixtures containing

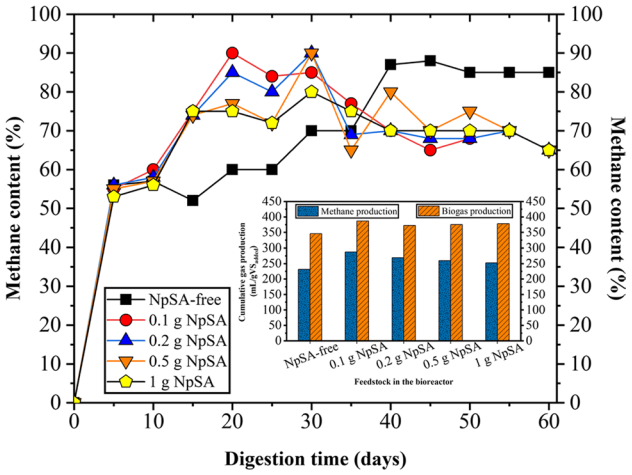

Fig. 4 Cumulative production and content of CH_4 for AnCD

NpSA was almost 1.5–2 times higher than the blank mixture between the 15th and 30th days of the experimental study. After the 35th day of the experimental study, the daily biogas production of mixtures containing NpSA began to decrease sharply, and the difference between them and the blank mixture began to close. The highest biogas production efficiency in 1 day between the 15th and 35th days of the experimental period was 52 mL/day, 43 mL/day, 38 mL/day, and 36 mL/day for bioreactors having 0.1 g, 0.2 g, 0.5 g, and 1 g NpSA, respectively. This value was 27 mL/day for the mixture without NpSA. As a matter of fact, the daily biogas production of the NpSA-free mixture continued in a more stable manner and thus, the gas production difference between the other bioreactors decreased until the 60th day.

As a result, it has been proven that biogas production will increase faster in the AD process by adding NpSA to the medium. This demonstrated that NpSA as an additive works as a catalyst. However, to achieve the highest level of biogas production, the amount of NpSA added to the bioreactor must be optimized for each study. Because, according to this study, although the presence of NpSA in the environment had a positive effect on biogas production, biogas production efficiency decreased as the NpSA dose in the mixture increased. The superiority of biogas production in bioreactors with NpSA added is attributed to the increase in the surface area to which anaerobic microorganisms that undertake the duty of gas production in AD and AnCD processes can adhere, thus increasing the flocculation possibilities of these microorganisms [18]. The high surface area of synthesized NpSA contributes to the attachment and rapid growth of anaerobic microorganisms, thus helping to reduce the microbial lag phase and increase biogas production [29]. In addition, the hydrophobic structure of NpSAs added to the bioreactor does not absorb the liquid in the environment; on the contrary, it pushes the liquid into the environment and contributes to the dissolution of organic substances in the environment [55]. This helps microorganisms digest monomerized organic substances more easily. However, it cannot be ignored that the rate of increase in biogas production decreases as the amount of NpSA in the environment increases. This can be attributed to the fact that as the abundance of NpSA in the bioreactor increases, the proportion of aerogel floating on the mixture increases due to its hydrophobic properties (SM-Fig. 1).

As the NpSA dose increased, the particles came together and formed a larger and rougher surface; thus, the movement of the liquid in the mixture (especially the movement of the liquid surface under the clustered NpSA particles in floating form) may have been prevented [56]. This may have prevented the homogeneous distribution of anaerobic microorganisms in the environment due to excessive adhesion to the NpSA surface, even if the bioreactors were mixed with a shaking incubator throughout the experiment. At this point, we suggest using a mechanical stirrer for pilot-scale studies where it is planned to add hydrophobic aerogel directly to the mixture in the bioreactor for catalyst purposes.

The cumulative methane production of NpSA-free mixture was 715.8 mL, corresponding to the lowest methane production achieved during the study as in biogas production efficiency. The cumulative methane production efficiencies of mixtures containing NpSA at least to the highest dose were 890.8 mL, 834.2 mL, 803.4 mL, and 781.1 mL, respectively. At the end of the 60-day experimental period, the methane production efficiency of the bioreactors containing NpSA increased by an average of 9–24% compared to blank mixture. Accordingly, in bioreactors containing 0.1 g, 0.2 g, and 0.5 g NpSA, an increase of 14%, 7%, and 3% was observed, respectively, compared to 0.5 g NpSA (20 gNpSA/L), where the lowest methane production occurred (excluding blank). Besides, it was determined that the average methane ratio in all bioreactors was in the range of 69–72%, but the methane ratio in each bioreactor was superior to each other on quite different days during the study. For example, although there was no significant difference in the methane content of the bioreactors in the first 10 days of the AD study, at the end of the 3rd week, the methane content of the blank mixture was 52%, while the CH_4 content of the mixtures containing NpSA was around 74–75%. The maximum methane content in the bioreactors was 90% recorded on day 20 for 0.1 g NpSA and on day 30 for 0.2 and 0.5 g NpSA. The methane content did not exceed 80% for 1 g of NpSA and the highest value was obtained on the 30th day. The lower methane content in the bioreactor containing more NpSA can be attributed to the increase in the aerogels in the environment and the increase in the surface area to which the microorganisms in the precursor stages (hydrolysis and acidogenesis) of the AD process can attach. As it is known, hydrolytic and acidogenic microorganisms

develop and reproduce faster than methanogens [57]. Then, the complex organics in the mixture decompose faster and increase the amount of dissolved organic matter in the environment, causing the pH value to decrease in the bioreactor and the accumulation of volatile fatty acids (VFAs) in the environment. Although the production of VFAs is a direct precursor for the final stage of methanogenesis, their accumulation in the bioreactor is reported as a cause of failure of AD [58]. However, the maximum methane content of the blank mixture reached 88% on day 45, showing a progression from low to high rate similar to that observed in common AD systems. In a way, this is proof that anaerobic microorganisms grow faster (in various AD stages) in bioreactors with NpSA. Moreover, today, hydrophobic aerogels are frequently preferred in the purification of biogas by adsorbing gases such as CO_2 [59, 60]. Gases such as CO_2 and H_2, which are formed faster and more in the environment because of the activities of acidogenic and acetogenic microorganisms, which increase in direct proportion to the dose of NpSA added to the bioreactors, may be adsorbed by the aerogels. This may cause the methane content in the produced biogas to be perceived as higher as the NpSA dose in the environment increases. These results obtained from the study showed that the use of NpSA could be an advantageous strategy to increase the methane content in biogas in a shorter time in anaerobic digestion processes. However, in addition to biogas production efficiency, it should be considered that systems with less NpSA content may be more efficient in terms of methane content. This is advantageous even considering the cost of NpSA synthesis and the labor involved in the production process.

Similarly, biogas production was achieved in bioreactors containing 1 g/L and 2 g/L silica gel by AnCD of water hyacinth and cow dung (7:3 w/w) (7% TS) in a semi-continuous system. Biogas production has been reported to increase by 35% and 15%, respectively, compared to the blank bioreactor. In addition, it was determined that the abundance of silica gel in the mixture and the biogas production were inversely proportional. However, at the end of the study, it was stated that the methane gas content (63–65%) of the bioreactors in which 1–6 g/L silica gel was added was quite similar to each other [61]. A more literature summary on the effect of different additives on AD and AnCD processes is given in Table 4.

3.3 Digestate characteristics

3.3.1 Organic material removal and pH change after AnCD

Dissolved COD, carbohydrate, protein, and total VS removal efficiency and final pH after AnCD are shown in Fig. 5. Moreover, digestate images and final characteristics are presented in the "supplementary material (SM. Figure 1 and SM. Table 2)." The balanced and stable pH value in the bioreactors during the AnCD has a significant effect on biogas and methane production. As it is known, optimum methane production generally occurs when the pH value in the bioreactor is around 6.5–8.5 [72]. At the end of the 60-day experimental period, the final pH of the digestates was determined to be between 7.52 and 7.82, supporting the efficient methane content in all bioreactors. It was observed that the lowest final pH was in the bioreactor with 1 g of NpSA added. The fact that the final pH of the NpSA additives below this value is quite similar to each other coincides with the later increase of the methane content of this bioreactor compared to the others (except NpSA-free). As mentioned before, the reason for this can be explained by the increase in the abundance of NpSA in the environment, the increase in anaerobic microorganisms, and the delay of the methanogenesis stage due to rapid organic matter hydrolysis (see Section 3.2). In addition, VS removal is another parameter that shows the capacity of methanogens to use dissolved organic substances in the environment. At the end of the study, it was determined that VS removal ranged from 34.59 to 54.44%, and the lowest removals were in NpSA-free and 1 g NpSA-containing bioreactors proportional to methane production rates. Dissolved protein removal rates for the AnCD process ranged from 43.62 to 65.33%. By increasing the NpSA ratio from 0.5 to 1 g in the mixture, the protein removal efficiency decreased by 33%. However, the protein removal efficiency of the mixtures containing 0.2 g and 0.5 g NpSA increased by an average of 15% compared to NpSA-free. Dissolved carbohydrate removal rates for the AnCD process were quite similar and ranged from 91.54 to 94.29%. This situation, in line with the literature, showed that anaerobic microorganisms can digest and prefer carbohydrates in the mixture more than proteins. This can generally be explained by the fact that there is a particular group that converts proteins in the AD and AnCD processes and this group has a slower growth rate than microorganisms that digest carbohydrates [73]. Dissolved COD removals after AnCD are determined as 69.66%, 71.21%, 70.79%, 52.81%, and 44.94% for NpSA-free, 0.1 g NpSA, 0.2 NpSA, 0.5 NpSA, and 1 g NpSA bioreactors, respectively. The lower sCOD removal in the bioreactors containing 1 g and 0.5 g NpSA compared to the others can be attributed to the fact that the aerogels, which are more abundant in the bioreactor, create more surface area for microorganisms to attach and grow. As a matter of fact, non-soluble organics that are hydrolyzed more rapidly in this way may have passed into the soluble form, increasing the initial sCOD value. The hydrolytic microorganisms, which got used to the ambient conditions over time, enabled sCOD to enter the process of removal in these bioreactors [74]. This has resulted in late methane production and low methane content.

Table 4 Literature summary on the effect of different additives on AD and AnCD processes

Material	Additive	Process conditions	Gas production		Ref
			Biogas	Methane	
Nanoparticle materials (metal elements and metal–metal oxide compounds)	Ni NPs	Batch reactor, C/N:25.5:1 Mesophilic temperature HRT: 50 days	1150.3 mL	676.9 mL	[62]
	Ag NPs	Batch reactor, C/N:6–16.5 Mesophilic temperature HRT: 55 days	–	0.341 L/g	[63]
	MnO_2 NPs	UASB reactor, 25–35 °C, HRT: 4 h days, C/N:6–16.5 L, active volume (AV): 60 mL	–	0.54 ± 0.02 mL/g VSS/h	[64]
	ZnO NPs	Batch reactor Mesophilic temperature HRT: 14 days, ZnO:15 mg/L	70 mL	–	[65]
	$MgCl_2$	Batch reactor Mesophilic temperature HRT: 30 days, AV:0.7 L, Inoculum: feed (I/F):2	–	~161 mL/g	[66]
Carbon based	Graphene	Batch reactor Mesophilic temperature HRT: 120 days, AV:0.3 L, I/F:0.7	–	180.5 mL/day	[67]
	Activated Carbon	Batch reactor Mesophilic temperature HRT: 59 days, C/N: 17.33 ± 0.02, AV:0.8 L, I/F:0.61–0.72	–	0.466 $L(gVS)^{-1}$ day^{-1}	[68]
	Biochar	Batch reactor, Mesophilic temperature, HRT: 100 days, C/N: 8.35, AV: 2 L	–	4.2 g VS/L/day	[69]
Composite material	Co/C	Batch reactor Mesophilic temperature, HRT: 35 days C/N:8.11 ± 0.14, AV: 0.5 L I/F: 2.33	585 mL/g VS	–	[70]
	CoO/C		576 mL/g VS	–	
	Co_3O_4/C		577 mL/g VS	–	

Table 4 (continued)

Material	Additive		Process conditions	Gas production		Ref
				Biogas	Methane	
Porous material	Silica gel		Batch reactor, Mesophilic temperature, HRT: 33 days, C/N:25, AV: 0.7 L	–	183 mL/L/day	[24]
	Slag		Batch reactor, Mesophilic temperature HRT: 60 days, 1 wt% blast furnace slag	399.4 mL/g VS	238.2 mL/g VS	[27]
	Zeolite		Batch reactor, Mesophilic temperature HRT: 60 days, AV: 1.64 L	–	~9 L/day	[71]
	Silica aerogel	0.1 g NPSA (2 g/L)	Industrial pomegranate waste/wastewater, and sewage sludge used as substrates Batch reactor Mesophilic temperature, HRT:60 days, AV: 0.05 L, 8% TS	1198.5 mL 387.2 mL/ gVS_{added}	287.8 mL/gVS_{added}	This study
		0.2 g NPSA (4 g/L)		1153.5 mL 372.7 mL/ gVS_{added}	269.5 mL/gVS_{added}	
		0.5 g NPSA (10 g/L)		1162.0 mL 375.4 mL/ gVS_{added}	259.6 mL/gVS_{added}	
		1 g NPSA (20 g/L)		1071 mL 378.4 mL/ gVS_{added}	252.4 mL/gVS_{added}	

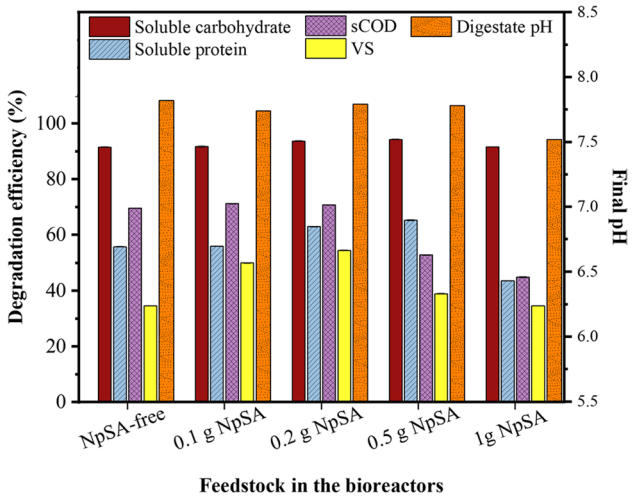

Fig. 5 Dissolved organic matter and VS removal efficiency and final pH of the digestates

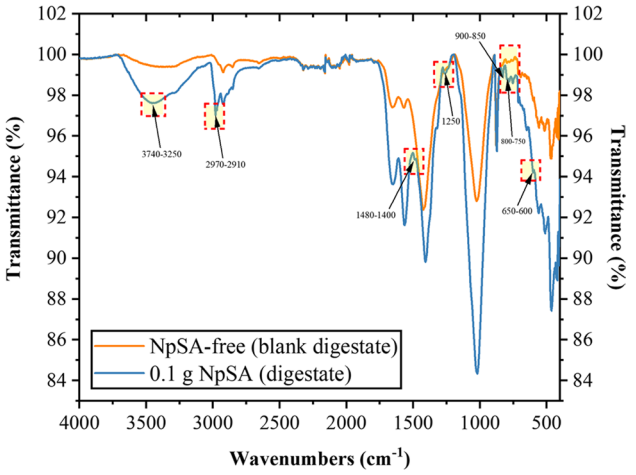

Fig. 6 FT-IR spectra of 0.1 g NpSA and NpSA-free digestates after AnCD

3.3.2 FTIR spectra of the digestates

The characteristic absorptions of synthesized NpSA were obtained before AnCD process (Fig. 2e). The characteristic absorptions of the digestate contain 0.1 g NpSA (the additive abundance which is the highest biogas and methane producer) and the digestate of blank bioreactor (NpSA-free) was obtained at the end of the AnCD process. As a result of the AnCD process, it was observed physically and visually that NpSA was not degraded in the digestates formed in the bioreactors to which NpSA was added and was still present in the form in which it was first added (SM. Figure 1). The main purpose of FT-IR analysis is to determine whether the NpSA in the digestate as a result of the AnCD process contains functional groups similar to the initial form in which it was synthesized, thus supporting the sustainable use of NpSA. The FTIR spectroscopy analysis of chosen digestates is given in Fig. 6. Absorption locations and corresponding functional groups of chosen digestates and synthetized NpSA are given in Table 5.

The spectrum shows a broad absorption band at 3000–3750 cm^{-1}, which is assigned to the O–H vibration of carboxylic and alcoholic groups and the peak with a center of ~ 3400 cm^{-1} represents hydrogen vibrations of alcohols, phenols, and organic acids [77]. In addition, due to the presence of hydroxyl groups (–OH) on the NpSA surface corresponds to the peak Si–OH bonds seen in the wavenumber range of 3740–3250 cm^{-1}. The peaks around 2970, 2850, and 1440 cm^{-1} represent the bending vibration of the C–H bonds in the $–CH_2$ and $–CH_3$ groups and the symmetrical C–H stretching vibrations in the CH_2 and CH_3 groups [78]. The peak seen at the wavenumber of 1250 cm^{-1} is attributed to Si–CH_3 bending which are found in the NpSA [79]. Si–O covalent bond vibrations are seen in the band range of 1000–1200 cm^{-1}. The peak at wavenumber 900–850 cm^{-1} is attributed to CH_3 rocking in Si–$(CH_3)_2$ [80]. The oxygen atoms act as a bridge between the two silicon atoms, proving a dense silica network [81]. The peaks, which are seen at ~825–707 cm^{-1} display a network Si–O–Si (vibrational bending) [82]. Also, the peak at 840–825 cm^{-1} displays three dimensional ≡Si–O–Si≡ aerogel network. The bands at ~478–460 cm^{-1} are assigned with a network of Si–O–Si bond (rocking modes of vibration) [83]. The peak seen in both digestates between 1560 and 1565 cm^{-1} were appropriate with the existence of carboxylate groups, especially acetate formed in the AnCD. Therefore, the band at 1560–1578 cm^{-1} is attributed to COO^- stretching vibrations [84]. The bands at 1020–1030 cm^{-1} are possibly due to C–O stretching [85]. As a result, it was determined that even in digestate containing as little as 0.1 g of NpSA, the synthesized NpSA had very similar functional groups. This may be evidence that NpSA, which is observed physically as a whole in the digestate, completes the AnCD process without degradation. In order to support the accuracy of this result, a detailed characterization analysis of NpSAs extracted from the digestate should be performed and the reusability of NpSAs during the AD process should also be investigated.

3.4 Kinetic study of cumulative methane production

Modified Gompertz (MG), logistic function (LF), and transference function (TF) models were applied to all experimental sets to obtain the optimum equation to fit abundance of NpSA additive and to determine the parameters associated with the AnCD process. Cumulative methane production and its fitted kinetic curves associated with the AnCD are presented in Fig. 7. The predicted values of the selected model

Table 5 Absorption locations and corresponding functional groups of synthesized NpSA and chosen digestates [75, 76]

Absorption locations			Corresponding functional group
Synthesized NpSA	NpSA-free digestate	0.1 g NpSA digestate	
3740–3250	–	3450	O–H stretching, Si–OH groups
2970–2910	–	2970	C–H stretching
–	2923	2923	C–H stretching
2850	2852	2852	Symmetrical C–H stretching
–	1650	1654	C = O stretching
–	1565	1560	COO^- stretching
1440	–	1440	C–H stretching
1250	–	1250	Si–R; $Si–CH_3$
–	1024	1027	C–O stretching
896	–	863	Si–R bending
793	–	781	Si–O vibrations
615	–	604	Si–O–Si stretching
–	–	468	Si–O–Si bending

–non-detected

parameters are shown in Table 6. In determining the kinetic model most fitted with the experimental results, it was considered that in addition to the high R^2 and low RMSE values, the error percentage between the experimental and model data in methane production should be less than 25% according to the literature [86]. It was stated that the most appropriate model for the estimation of methane production was LF. Model-fitting data relevance was followed by TF and MG, respectively. S-shaped sigmoid curves, also called growth curves, represent the increase in growth rate and cumulative methane yield of methanogens in accordance with kinetic models such as LG and MG. Over time, the growth rate of the microorganism responsible for methane production slows down and eventually reaches an asymptote corresponding to zero [85]. When Table 6 is examined, it is observed that 0.1 g NpSA bioreactor (best methane production in the study) and NpSA-free bioreactors are more compatible with MG than other bioreactors. The reason for this is that although the addition of NpSA to the mixture increases biogas production, it restricts the development of methanogens as their abundance in the environment increases. This situation is compatible with both biogas and methane production values obtained by the experimental study.

The lag phase constant (λ) defines the time required for anaerobic microorganisms to acclimate to the system. Considering LF, which is the model most compatible with the experimental results, it is seen that the "λ" value decreases as the NpSA ratio in the mixture increases. This is consistent with the overall study because, as mentioned before, NpSA with a large surface area constitutes the necessary attachment environment for the growth and development of microorganisms. This facilitated both the physical growth (size) of microorganisms and their proliferation in the environment as NpSA increased [87]. As a result, the hydrolysis of organic matters in the bioreactors was also accelerated and this triggered the formation of more VFAs in the bioreactors.

3.5 Possible energy efficiency and economic evaluation

The most important advantage of such biomass processing systems, in addition to controlled waste disposal, is the amount of green energy that can be obtained by methane production. However, in AD studies where additives are used to enhance biogas/methane production, if the synthesis or direct purchase cost of the additive is not considered, it is not possible to make a proper and reliable economic evaluation based on energy gain. In this part of the study, it is discussed how profitable the mixtures with NpSA additives in various abundances are compared to NpSA-free. For this purpose, the gain from the cost of electricity consumption by converting the amount of methane produced from each experimental set into electrical energy, as well as the estimated financial gain from the sale of methane directly by storing it, was investigated. Detailed energy conversion and economic analysis are given in the "supplementary material (SM. Table 3)."

For this study, it was determined that the mixture with the best energy output potential in proportion to the best methane production was in the bioreactor containing 0.1 g NpSA and that 0.00286 kWh/gVS (2.86 kWh/kgVS) of energy could be produced with this additive abundance. In addition, the NpSA-free bioreactor can also produce 0.00230 kWh/gVS (2.30 kWh/kgVS) energy. For this

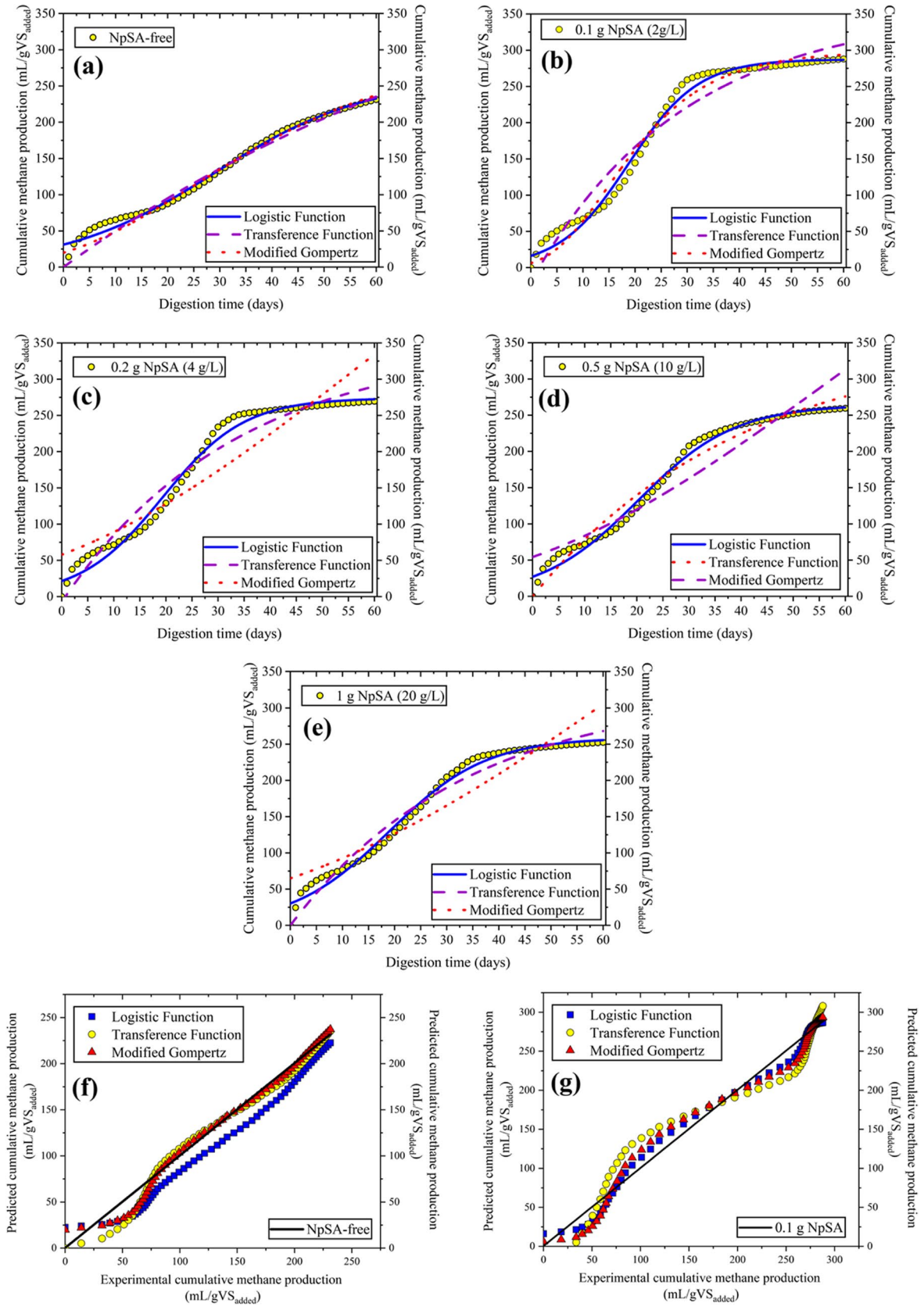

Fig. 7 Cumulative methane production and its fitted kinetic curves (**a**) NpSA-free, (**b**) 0.1 g NpSA, (**c**) 0.2 g NpSA, (**d**) 0.5 g NpSA, (**e**) 1 g NpSA and cumulative experimental-predicted methane production for models of chosen bioreactors (**f**) NpSA-free and (**g**) 0.1 g NpSA

Table 6 Kinetic parameters of average cumulative methane production curves

Model	Parameter	NpSA-free	0.1 g NpSA	0.2 g NpSA	0.5 g NpSA	1 g NpSA
Modified Gompertz	$C(t)$-Exp. (mL/gVS)	231.26	287.81	269.51	259.58	252.39
	$C(t)$-Pre. (mL/gVS)	237.27	293.62	333.59	312.59	305.03
	Diffe. exp. and pre. (%)	2.5	1.9	19	17	17
	U (mL/gVS)	301.05	297.98	876.40	822.68	982.33
	Rb	4.49	10.18	5.56	5.21	5.08
	n	0	3.84	0	0	0
	R^2	0.9844	0.9787	0.8463	0.8920	0.8726
	RMSE	8.23	14.13	34.58	26.60	27.62
Transference function	$C(t)$-Exp. (mL/gVS)	231.26	287.81	269.51	259.58	252.39
	$C(t)$-Pre. (mL/gVS)	235.12	308.089	290.13	275.81	268.02
	Diffe. exp. and pre. (%)	1.7	6.8	7.1	5.8	5.8
	U (mL/gVS)	510.95	356.66	349.84	355.21	322.66
	λ (d)	0	1.57	0.69	0	0
	Rb	5.25	12.17	10.43	8.87	9.55
	R^2	0.9756	0.9475	0.9524	0.9704	0.9683
	RMSE	10.32	22.18	19.24	13.92	13.75
Logistic function	$C(t)$-Exp. (mL/gVS)	231.26	287.81	269.51	259.58	252.39
	$C(t)$-Pre. (mL/gVS)	222.67	286.69	272.24	260.61	255.56
	Diffe. exp. and pre. (%)	3.8	0.38	1	0.39	1.2
	U (mL/gVS)	260.20	287.28	273.79	264.25	258.71
	λ (d)	5.13	5.44	3.67	1.59	0.24
	Rb	4.48	10.77	8.71	7.09	6.92
	R^2	0.9900	0.9903	0.9869	0.9908	0.9896
	RMSE	19.23	9.51	10.08	7.74	7.86

study, the approximate cost of 1 g of NpSA synthesis was determined as $1.54 (above the market due to the quality chemicals used in synthesis). In this case, it has been calculated that no methane-energy conversion of any bioreactor with NpSA added will be profitable. The synthesis cost increases depending on the amount of NpSA added to the mixtures, which remains above the financial gain of electrical energy that can be obtained from the biogas produced in the reactors. As a result, only the NpSA-free bioreactor can generate a profit of about $\$0.024/L_{mixture}$ when electrical energy conversion is considered. Similarly, it was reported that 0.72 kWh/kgVS energy can be obtained in return for the produced methane as a result of the AnCD of various organic wastes (citrus, fertilizer, whey, etc.) that do not contain any additives in 2018 [88].

However, when the profit that can be obtained from the sale of the produced methane directly in the global market is calculated in the study, it has been determined that 0.1 g NpSA bioreactor can bring a profit of $\$1.4/L_{mixture}$ compared to NpSA-free (even when the necessary NpSA synthesis cost is subtracted from the methane sales profit). Other bioreactors with NpSA added could not gain financial profit due to the required NpSA synthesis cost compared to NpSA-free. In this case, based on this study, the fact that the most efficient methane production was realized in the bioreactor with the lowest NpSA contribution was economically very beneficial.

3.6 Possible environmental implications

Fossil fuel, which provides approximately 80% of the total energy consumed annually, is the dominant energy source in the world today [89]. However, many negative environmental effects of fossil fuel consumption are known, such as global warming, acid rain, water and air pollution, and desertification, etc. At this point, it is thought that the low-cost energy obtained from biomass can largely meet the energy demand of the increasing population all over the world, and waste-related environmental pollution can be prevented, especially by using domestic and industrial organic waste, as in this study. In addition, in this study, rice husk ash, which is classified as agro-industrial waste, was used as a precursor in silica aerogel synthesis, thus reducing the NpSA production cost. Moreover, instead of the supercritical drying method used in traditional applications of the sol–gel method, which has hazardous effects on the environment and human health, the drying process in the ambient atmosphere, which is more sustainable and environmentally friendly, was

preferred. It has been shown that the addition of the synthesized hydrophobic nanoporous silica aerogel to the AD and AnCD processes can increase the methane content, which reveals the quality of the produced biogas, and the formation rate of methane in the AD process. In addition, according to the results of this study, it was observed that low-dose NpSA additive increased the biogas and methane production potential more than high doses. Although it has been observed that the silica aerogels used in the AD process are visually and structurally (chemical bond) similar to the initial state in which they were synthesized, their reusability requires further research.

4 Conclusion

The hydrophobic NpSA additive was effective to improve the AnCD performance, biogas/methane production, and organic matter removal of organic waste mixture from fruit industry waste and sewage sludge. A dose of 0.1 g NpSA (0.03 g/gVS) had a 12% and 24% increase in biogas and methane production, and 45% more VS removal, respectively, than NpSA-free. As the abundance of NpSA in the mixture increased, the biogas and methane production efficiency started to decrease, although still higher than NpSA-free. This is because with increasing NpSA, anaerobic microorganism access more surface area to grow and hydrolyze organic materials faster, causing VFA to accumulate in the bioreactor. However, at the NpSA abundances studied, no inhibition from acidification occurred, as AnCD systems managed to recover. Experimental results fitted the LF, TF, and MG kinetic models in order of success. It has been determined that with the sale of the produced methane directly in the global energy market, 0.1 g NpSA additive can provide 1.4 $\$/L_{mixture}$ more financial gain than the mixture without NpSA.

Supplementary Information The online version contains supplementary material available at https://doi.org/10.1007/s13399-024-05566-6.

Author contribution Habibe Elif GULSEN AKBAY: mainly in anaerobic digestion studies; methodology, conceptualization, investigation, formal analysis, data curation, validation, visualization, writing—original draft.

Oykum BASGOZ: mainly in additive material synthesis; data curation, investigation, methodology, formal analysis, validation, writing—original draft.

Omer GULER: mainly in additive material synthesis; supervision, validation, resources, conceptualization.

All authors aided in interpreting the results, worked on the manuscript, discussed the results, and commented on the manuscript. All authors are approving the final version of the manuscript.

Funding Open access funding provided by the Scientific and Technological Research Council of Türkiye (TÜBİTAK).

Data availability The datasets used and/or analyzed during the current study are available from the corresponding author on reasonable request.

Declarations

Ethical approval Not applicable.

Consent to participate All the authors of this article are consented to participate.

Competing interests The authors declare no competing interests.

References

1. U.S. Energy Information Administration (2010) International Energy Outlook, 2010. Washington, DC
2. Song Y, Pei L, Chen G et al (2023) Recent advancements in strategies to improve anaerobic digestion of perennial energy grasses for enhanced methane production. Sci Total Environ 861:160552. https://doi.org/10.1016/J.SCITOTENV.2022.160552
3. Chovau S, Degrauwe D, Van Der Bruggen B (2013) Critical analysis of techno-economic estimates for the production cost of lignocellulosic bio-ethanol. Renew Sustain Energy Rev 26:307–321. https://doi.org/10.1016/j.rser.2013.05.064
4. Kılıç Depren S, Kartal MT, Çoban Çelikdemir N, Depren Ö (2022) Energy consumption and environmental degradation nexus: a systematic review and meta-analysis of fossil fuel and renewable energy consumption. Ecol Inform 70:101747. https://doi.org/10.1016/J.ECOINF.2022.101747
5. Danish WZ (2019) Does biomass energy consumption help to control environmental pollution? Evidence from BRICS countries. Sci Total Environ 670:1075–1083. https://doi.org/10.1016/J.SCITOTENV.2019.03.268
6. Pinto S, Jamshidi Far A, Dionisi D (2021) Land and water requirements for the supply of renewable heating and transport energy using anaerobic digestion and water electrolysis A case study for the UK. Sustain Energy Technol Assessments 48:101636. https://doi.org/10.1016/J.SETA.2021.101636
7. Pensini A, Rasmussen CN, Kempton W (2014) Economic analysis of using excess renewable electricity to displace heating fuels. Appl Energy 131:530–543. https://doi.org/10.1016/J.APENERGY.2014.04.111
8. Parvathy Eswari A, Ravi YK, Kavitha S, Rajesh Banu J (2023) Recent insight into anaerobic digestion of lignocellulosic biomass for cost effective bioenergy generation. e-Prime-Adv Electr Eng Electron Energy 3:100119. https://doi.org/10.1016/J.PRIME.2023.100119

9. Chen Q, Zhao B, Zhang Y et al (2023) The function of "Cambi® thermal hydrolysis + anaerobic digestion" on heavy metal behavior and risks in a full-scale sludge treatment plant based on four seasons investigation. J Hazard Mater 445:130579. https://doi.org/10.1016/J.JHAZMAT.2022.130579
10. Leitão A, Moni D, Maria C (2022) Anaerobic co-digestion of food waste with sewage sludge from wastewater treatment plant of Sequele Luanda-Angola. Environ Challenges 9:100635. https://doi.org/10.1016/J.ENVC.2022.100635
11. He D, Zheng S, Xiao J et al (2022) Effect of lignin on short-chain fatty acids production from anaerobic fermentation of waste activated sludge. Water Res 212:118082. https://doi.org/10.1016/J.WATRES.2022.118082
12. Appels L, Baeyens J, Degrève J, Dewil R (2008) Principles and potential of the anaerobic digestion of waste-activated sludge. Prog Energy Combust Sci 34:755–781. https://doi.org/10.1016/J.PECS.2008.06.002
13. Liu H, Wang X, Fang Y et al (2022) Enhancing thermophilic anaerobic co-digestion of sewage sludge and food waste with biogas residue biochar. Renew Energy 188:465–475. https://doi.org/10.1016/J.RENENE.2022.02.044
14. Koyama M, Yamamoto S, Ishikawa K et al (2017) Inhibition of anaerobic digestion by dissolved lignin derived from alkaline pre-treatment of an aquatic macrophyte. Chem Eng J 311:55–62. https://doi.org/10.1016/J.CEJ.2016.11.076
15. Chiappero M, Berruti F, Mašek O, Fiore S (2021) Analysis of the influence of activated biochar properties on methane production from anaerobic digestion of waste activated sludge. Biomass Bioenergy 150:106129. https://doi.org/10.1016/J.BIOMBIOE.2021.106129
16. Zhao J, Hou T, Wang Q et al (2021) Application of biogas recirculation in anaerobic granular sludge system for multifunctional sewage sludge management with high efficacy energy recovery. Appl Energy 298:117212. https://doi.org/10.1016/J.APENERGY.2021.117212
17. Wang X, Jiang C, Wang H et al (2023) Strategies for energy conversion from sludge to methane through pretreatment coupled anaerobic digestion: potential energy loss or gain. J Environ Manage 330:117033. https://doi.org/10.1016/J.JENVMAN.2022.117033
18. Liu M, Wei Y, Leng X (2021) Improving biogas production using additives in anaerobic digestion: a review. J Clean Prod 297:126666. https://doi.org/10.1016/J.JCLEPRO.2021.126666
19. Rowan M, Umenweke GC, Epelle EI et al (2022) Anaerobic co-digestion of food waste and agricultural residues: an overview of feedstock properties and the impact of biochar addition. Digital Chem Eng 4:100046. https://doi.org/10.1016/J.DCHE.2022.100046
20. Romero-Güiza MS, Vila J, Mata-Alvarez J et al (2016) The role of additives on anaerobic digestion: a review. Renew Sustain Energy Rev 58:1486–1499. https://doi.org/10.1016/j.rser.2015.12.094
21. Yang Y, Tada C, Miah MS et al (2004) Influence of bed materials on methanogenic characteristics and immobilized microbes in anaerobic digester. Mater Sci Eng, C 24:413–419. https://doi.org/10.1016/J.MSEC.2003.11.005
22. Garcia ML, Lapa KR, Foresti E, Zaiat M (2008) Effects of bed materials on the performance of an anaerobic sequencing batch biofilm reactor treating domestic sewage. J Environ Manage 88:1471–1477. https://doi.org/10.1016/J.JENVMAN.2007.07.015
23. Milán Z, Villa P, Sánchez E et al (2003) Effect of natural and modified zeolite addition on anaerobic digestion of piggery waste. Water Sci Technol 48:263–269. https://doi.org/10.2166/WST.2003.0411
24. Adu-Gyamfi N, Ravella SR, Hobbs PJ (2012) Optimizing anaerobic digestion by selection of the immobilizing surface for enhanced methane production. Bioresour Technol 120:248–255. https://doi.org/10.1016/J.BIORTECH.2012.06.042
25. Abdelwahab TAM, Mohanty MK, Sahoo PK, Behera D (2023) Metal nanoparticle mixtures to improve the biogas yield of cattle manure. Biomass Convers Biorefin 13:2243–2254. https://doi.org/10.1007/S13399-021-01286-3/TABLES/6
26. Çalhan R, Ulutaş K (2023) Boosting biogas production and methane yield by using street dust as an additive on anaerobic digestion of cattle manure. Biomass Convers Biorefin 13:7385–7396. https://doi.org/10.1007/S13399-023-04231-8/TABLES/5
27. Canan A, Calhan R, Ozkaymak M (2021) Investigation of the effects of different slags as accelerant on anaerobic digestion and methane yield. Biomass Convers Biorefin 11:1395–1406. https://doi.org/10.1007/S13399-021-01340-0/FIGURES/5
28. Khashaba NH, Ettouney RS, Abdelaal MM et al (2022) Artificial neural network modeling of biochar enhanced anaerobic sewage sludge digestion. J Environ Chem Eng 10:107988. https://doi.org/10.1016/J.JECE.2022.107988
29. Picanço AP, Vallero MVG, Gianotti EP et al (2001) Influence of porosity and composition of supports on the methanogenic biofilm characteristics developed in a fixed bed anaerobic reactor. Water Sci Technol 44:197–204. https://doi.org/10.2166/WST.2001.0220
30. Breitenbucher K, Siegl M, Knupfer A, Radke M (1990) Open-pore sintered glass as a high-efficiency support medium in bioreactors: new results and long-term experiences achieved in high-rate anaerobic digestion. Water Sci Technol 22:25–32. https://doi.org/10.2166/WST.1990.0133
31. Rékási M, Ragályi P, Sándor DB et al (2023) Effect of composting and vermicomposting on potentially toxic element contents and bioavailability in sewage sludge digestate. Bioresour Technol Rep 21:101307. https://doi.org/10.1016/J.BITEB.2022.101307
32. Alves MM, Pereira Alcina M, Novais Maggiolly J, Polanco Fdz F, Mota M (1999) A new device to select microcarriers for biomass immobilization: application to an anaerobic consortium. Water Environ Res 71:2. https://doi.org/10.2175/106143098X121824
33. Sun M, Bu Y, Xin X, Feng J (2022) Polyurethane functionalized silica aerogel for in-tube solid-phase microextraction of estrogens prior to high performance liquid chromatography detection. Microchem J 181:107699. https://doi.org/10.1016/J.MICROC.2022.107699
34. Li C, Liu Q, Zhang G et al (2023) Rapid synthesis of MTES-derived silica aerogel monoliths in Cetyltrimethylammonium bromide/water solvent system by ambient pressure drying. Powder Technol 418:118314. https://doi.org/10.1016/J.POWTEC.2023.118314
35. Lima D, Appleby G, Li L (2023) A scoping review of options for increasing biogas production from sewage sludge: challenges and opportunities for enhancing energy self-sufficiency in wastewater treatment plants. Energies 16:2369. https://doi.org/10.3390/EN16052369
36. Gulsen Akbay HE, Kumbur H (2018) Investigation of biogas production potential of fruit wastes and sewage sludge by co-digestion method. Int J Sci Technol Educ Res 4:8
37. Leme MAG, Torres-Mayanga PC, Lachos-Perez D et al (2022) Biogas production from the landfilled easily degradable fraction of municipal solid waste: mining strategy for energy recovery. Biomass Convers Biorefin 1:1. https://doi.org/10.1007/S13399-022-03264-9
38. Gulsen Akbay HE, Dizge N, Kumbur H (2021) Enhancing biogas production of anaerobic co-digestion of industrial waste and municipal sewage sludge with mechanical, chemical, thermal, and hybrid pretreatment. Bioresour Technol 340:125688. https://doi.org/10.1016/J.BIORTECH.2021.125688
39. Abdel-Hadi MA (2008) A simple apparatus for biogas quality determination. Misr J Ag Eng 25:1055–1066

40. Gulsen Akbay HE (2024) Anaerobic mono and co-digestion of agro-industrial waste and municipal sewage sludge: biogas production potential, kinetic modelling, and digestate characteristics. Fuel 355:129468. https://doi.org/10.1016/J.FUEL.2023.129468
41. US Environmental Protection Agency (1996) Method 2540B and 2540E, Test Methods for Eva2001ing Solid Waste Physical/Chemical Methods SW-846, 3r
42. US Environmental Protection Agency (2001) Method 1684, total, fixed, and volatile solids in water, solids, and biosolids U.S. EPA
43. US Environmental Protection Agency (2004) Method 9045D, soil and waste pH, part of test methods for evaluating solid waste, physical/chemical methods. In: Hazardous Waste Test Methods / SW-846 pp 1–5
44. American Public Health Association (1995) Standard Methods for the Examination of Water and Wastewater, 16th edn. Washington
45. Dubois M, Gilles KA, Hamilton JK et al (1956) Colorimetric method for determination of sugars and related substances. Anal Chem 28:350–356
46. Lowry OH, Rosebrough NJ, Farr AL, Randall RJ (1951) Protein measurement with the Folin phenol reagent. J Biol Chem 193:265–275. https://doi.org/10.1016/s0021-9258(19)52451-6
47. Wang S, Wang J, Li J et al (2021) Evaluation of biogas production potential of trace element-contaminated plants via anaerobic digestion. Ecotoxicol Environ Saf 208:111598. https://doi.org/10.1016/J.ECOENV.2020.111598
48. Kainthola J, Shariq M, Kalamdhad AS, Goud VV (2019) Enhanced methane potential of rice straw with microwave assisted pretreatment and its kinetic analysis. J Environ Manage 232:188–196. https://doi.org/10.1016/j.jenvman.2018.11.052
49. Deepanraj B, Sivasubramanian V, Jayaraj S (2015) Experimental and kinetic study on anaerobic digestion of food waste: the effect of total solids and pH. J Renew Energy 7:063104. https://doi.org/10.1063/1.4935559
50. Pramanik SK, Suja FB, Porhemmat M, Pramanik BK (2019) Performance and kinetic model of a single-stage anaerobic digestion system operated at different successive operating stages for the treatment of food waste. Processes 7:600. https://doi.org/10.3390/PR7090600
51. Gulsen Akbay HE, Dizge N, Kumbur H (2022) Evaluation of electro-oxidation and Fenton pretreatments on industrial fruit waste and municipal sewage sludge to enhance biogas production by anaerobic co-digestion. J Environ Manage 319:115711. https://doi.org/10.1016/J.JENVMAN.2022.115711
52. Electricity prices around the world, GlobalPetrolPrices.com. https://www.globalpetrolprices.com/electricity_prices/. Accessed 18 May 2023
53. Methane prices around the world, GlobalPetrolPrices.com. https://www.globalpetrolprices.com/methane_prices/. Accessed 18 May 2023
54. Salam B, Biswas S, Rabbi MS (2015) Biogas from mesophilic anaerobic digestion of cow dung using silica gel as catalyst. Procedia Eng 105:652–657. https://doi.org/10.1016/J.PROENG.2015.05.044
55. Štandeker S, Novak Z, Knez Ž (2007) Adsorption of toxic organic compounds from water with hydrophobic silica aerogels. J Colloid Interface Sci 310:362–368. https://doi.org/10.1016/J.JCIS.2007.02.021
56. Rao AV, Kulkarni MM, Bhagat SD (2005) Transport of liquids using superhydrophobic aerogels. J Colloid Interface Sci 285:413–418. https://doi.org/10.1016/J.JCIS.2004.11.033
57. Deublein D, Steinhauser A (2008) Biogas from waste and renewable resources. Biogas from Waste and Renew Resourhttps://doi.org/10.1002/9783527621705
58. Akuzawa M, Hori T, Haruta S et al (2011) Distinctive responses of metabolically active microbiota to acidification in a thermophilic anaerobic digester. Microb Ecol 61:595–605. https://doi.org/10.1007/S00248-010-9788-1
59. Zhang Z, Fei Z, Zhao S et al (2023) Enhanced CO2 adsorption property of amine in-situ hybrid SiO2 aerogels by the incorporation of micropores. Mater Lett 337:133942. https://doi.org/10.1016/J.MATLET.2023.133942
60. Dolbin AV, Khlistyuck MV, Esel'Son VB et al (2018) Sorption of hydrogen by silica aerogel at low-temperatures. Low Temp Phys 44:144. https://doi.org/10.1063/1.5020910
61. Patel V, Patel A, Datta M (1992) Effects of adsorbents on anaerobic digestion of water hyacinth - cattle dung. Bioresour Technol 40:179–181. https://doi.org/10.1016/0960-8524(92)90206-D
62. Abdelsalam E, Samer M, Attia YA et al (2017) Effects of Co and Ni nanoparticles on biogas and methane production from anaerobic digestion of slurry. Energy Convers Manag 141:108–119. https://doi.org/10.1016/J.ENCONMAN.2016.05.051
63. Grosser A, Grobelak A, Rorat A et al (2021) Effects of silver nanoparticles on performance of anaerobic digestion of sewage sludge and associated microbial communities. Renew Energy 171:1014–1025. https://doi.org/10.1016/j.renene.2021.02.127
64. Tian T, Qiao S, Yu C, Zhou J (2019) Effects of nano-sized MnO_2 on methanogenic propionate and butyrate degradation in anaerobic digestion. J Hazard Mater 364:11–18. https://doi.org/10.1016/J.JHAZMAT.2018.09.081
65. Luna-delRisco M, Orupõld K, Dubourguier HC (2011) Particle-size effect of CuO and ZnO on biogas and methane production during anaerobic digestion. J Hazard Mater 189:603–608. https://doi.org/10.1016/J.JHAZMAT.2011.02.085
66. Yuan T, Cheng Y, Wang X et al (2019) A novel anaerobic digestion system coupling biogas recirculation with MgCl2 addition for multipurpose sewage sludge treatment. J Clean Prod 230:499–507. https://doi.org/10.1016/J.JCLEPRO.2019.05.124
67. Zhu H, Han Y, Ma W et al (2018) New insights into enhanced anaerobic degradation of coal gasification wastewater (CGW) with the assistance of graphene. Bioresour Technol 262:302–309. https://doi.org/10.1016/J.BIORTECH.2018.04.080
68. Zhang L, Zhang J, Loh KC (2018) Activated carbon enhanced anaerobic digestion of food waste - laboratory-scale and pilot-scale operation. Waste Manag 75:270–279. https://doi.org/10.1016/J.WASMAN.2018.02.020
69. Yu Q, Sun C, Liu R et al (2021) Anaerobic co-digestion of corn stover and chicken manure using continuous stirred tank reactor: the effect of biochar addition and urea pretreatment. Bioresour Technol 319:124197. https://doi.org/10.1016/J.BIORTECH.2020.124197
70. Chen J, Yun S, Shi J et al (2020) Role of biomass-derived carbon-based composite accelerants in enhanced anaerobic digestion: focusing on biogas yield, fertilizer utilization, and density functional theory calculations. Bioresour Technol 307:123204. https://doi.org/10.1016/J.BIORTECH.2020.123204
71. Fernández N, Montalvo S, Fernández-Polanco F et al (2007) Real evidence about zeolite as microorganisms immobilizer in anaerobic fluidized bed reactors. Process Biochem 42:721–728. https://doi.org/10.1016/J.PROCBIO.2006.12.004
72. Valença RB, dos Santos LA, Firmo ALB et al (2021) Influence of sodium bicarbonate (NaHCO3) on the methane generation potential of organic food waste. J Clean Prod 317:128390. https://doi.org/10.1016/J.JCLEPRO.2021.128390
73. Deng Z, Ferreira ALM, Spanjers H, Van Lier JB (2022) Characterization of microbial communities in anaerobic acidification reactors fed with casein and/or lactose. Appl Microbiol Biotechnol Citation. https://doi.org/10.1007/s00253-022-12132-5
74. Bertucci M, Calusinska M, Goux X, et al (2019) Carbohydrate hydrolytic potential and redundancy of an anaerobic digestion microbiome exposed to acidosis, as uncovered by

metagenomics. Appl Environ Microbiol 85. https://doi.org/10.1128/AEM.00895-19
75. IR Spectrum Table. https://www.sigmaaldrich.com/TR/en/technical-documents/technical-article/analytical-chemistry/photometry-and-reflectometry/ir-spectrum-table. Accessed 14 May 2023
76. Roccotelli A, Araniti F, Tursi A et al (2020) Organic matter characterization and phytotoxic potential assessment of a solid anaerobic digestate following chemical stabilization by an iron-based fenton reaction. J Agric Food Chem 68:9461–9474. https://doi.org/10.1021/acs.jafc.0c03570
77. Cuetos MJ, Morán A, Otero M, Gómez X (2009) Anaerobic co-digestion of poultry blood with OFMSW: FTIR and TG-DTG study of process stabilization. Environ Technol 30:571–582. https://doi.org/10.1080/09593330902835730
78. Karamikamkar S, Karamikamkar S, Fashandi M et al (2020) In situ interface design in graphene-embedded polymeric silica aerogel with organic/inorganic hybridization. ACS Appl Mater Interfaces 12:26635–26648. https://doi.org/10.1021/ACSAMI.0C04531
79. Ito H, Onitsuka S, Gappa R et al (2013) Fabrication of amorphous silicon carbide films from decomposition of tetramethylsilane using ECR plasma of Ar. J Phys Conf Ser 441:012039. https://doi.org/10.1088/1742-6596/441/1/012039
80. Kapica R, Markiewicz J, Tyczkowska-Sieroń E et al (2020) Artificial superhydrophobic and antifungal surface on goose down by cold plasma treatment. Coatings 10:904. https://doi.org/10.3390/COATINGS10090904
81. Ambrozewicz D, Ciesielczyk F, Nowacka M, et al (2013) Fluoroalkylsilane versus alkylsilane as hydrophobic agents for silica and silicates. J Nanomater https://doi.org/10.1155/2013/631938
82. Shahrokh Abadi MH, Delbari A, Fakoor Z, Baedi J (2014) Effects of annealing temperature on infrared spectra of SiO_2 extracted from rice husk. J Ceram Sci Technol 6:41–46. https://doi.org/10.4416/JCST2014-00028
83. Babu BC, Naresh V, Prakash BJ, Buddhudu S (2011) Structural, thermal and dielectric properties of lithium zinc silicate ceramic powders by sol-gel method. 38:114–127. https://doi.org/10.1080/07315171.2011.623610
84. Bullen HA, Oehrle SA, Bennett AF et al (2008) Use of attenuated total reflectance fourier transform infrared spectroscopy to identify microbial metabolic products on carbonate mineral surfaces. Appl Environ Microbiol 74:4553–4559. https://doi.org/10.1128/AEM.02936-07
85. Zwietering MH, Jongenburger I, Rombouts FM, Van't Riet K (1990) Modeling of the bacterial growth curve. Appl Environ Microbiol 56:1875. https://doi.org/10.1128/AEM.56.6.1875-1881.1990
86. Kainthola J, Kalamdhad AS, Goud VV, Goel R (2019) Fungal pretreatment and associated kinetics of rice straw hydrolysis to accelerate methane yield from anaerobic digestion. Bioresour Technol 286:121368. https://doi.org/10.1016/j.biortech.2019.121368
87. López Velarde Santos M, Ventura Ramos E Jr Rodríguez Morales JA et al (2020) Effect of inoculum source on the anaerobic digestion of Mezcal Vinasses at different substrate-inoculum ratios. Rev Int Contam Ambient 36:81-95 https://doi.org/10.20937/RICA.2020.36.53276
88. Valenti F, Zhong Y, Sun M et al (2018) Anaerobic co-digestion of multiple agricultural residues to enhance biogas production in southern Italy. Waste Manage 78:151–157. https://doi.org/10.1016/J.WASMAN.2018.05.037
89. Afraz M, Muhammad F, Nisar J et al (2024) Production of value added products from biomass waste by pyrolysis: an updated review. Waste Management Bulletin 1:30–40. https://doi.org/10.1016/J.WMB.2023.08.004